Submitted to *Transportation Science*
manuscript (Please, provide the mansucript number!)

Dynamic Continuum Model with Elastic Demand for a Polycentric Urban City

Yan-Qun Jiang
Department of Mathematics, Southwest University of Science and Technology, Mianyang, Sichuan, China,
jyq2005@mail.ustc.edu.cn

S.C. Wong
Department of Civil Engineering, The University of Hong Kong, Hong Kong, China,
hhecwsc@hku.hk

Peng Zhang
Shanghai Institute of Applied Mathematics and Mechanics, Shanghai University, Shanghai, China,
pzhang@mail.shu.edu.cn

Keechoo Choi
Department of Transportation Engineering, TOD-based Sustainable Urban Transportation Center, Ajou University, Republic of Korea,
keechoo@ajou.ac.kr

This paper presents the development of a macroscopic dynamic traffic assignment (DTA) model for continuum transportation systems with elastic demand. A reactive dynamic user equilibrium model is extended to simulate network equilibrium problems for an urban area with multiple central business districts (CBDs). Each copy of traffic flow makes route choice decisions in a reactive manner to minimize the total travel cost from origin to destination, based on instantaneous traffic information from a radio broadcasting service or route guidance system. The elastic demand function for each copy of flow is associated with its total instantaneous travel cost. The model is solved by a cell-centered finite volume method for conservation law equations and a fast sweeping method for Eikonal-type equations on unstructured grids. Numerical experiments for an urban traffic network with two CBDs are presented to verify the rationality of the model and the validity of the numerical method. The numerical results indicate that the model captures some macroscopic characteristics of two copies of flow interacting in time-varying urban transportation systems, e.g., the spatial distributions of the flow density and flux and the path choice behavior in response to elastic demand, and can describe traffic equilibrium phenomena, such as self-organization and traffic congestion build-up and dissipation.

Key words: polycentric urban area; reactive dynamic user equilibrium; elastic demand; self-organization; traffic congestion; unstructured meshes
History:

1. Introduction

Dynamic traffic assignment (DTA), a generalization of static traffic assignment, plays an important role in traffic control and management. DTA models use time-varying traffic flow to capture traffic dynamics. They can be used in offline transportation planning and policy evaluation and in real-

time traffic management. The models are classified as dynamic user-optimal (DUO) models and dynamic system-optimal (DSO) models according to their different assignment patterns. In DUO models, the route choice behavior of travelers is based on the assumption that each user is self-interested and will always travel along the least time/cost path (Wie et al. 1990, Lam and Huang 1995, Boyce et al. 1995, Li et al. 2000, Nagurney and Dong 2002, Friesz et al. 2010, Xu et al. 2014, Hoogendoorn and Bovy 2004, Xia et al. 2008, Huang et al. 2009, Jiang et al. 2009, 2012, Du et al. 2013, Balijepalli et al. 2014, Chow et al. 2015, Levin et al. 2015). There are two DUO assignment patterns (Tong and Wong 2000): the reactive dynamic user-optimal (RDUO) assignment, in which a user chooses a route that minimizes his/her instantaneous travel time/cost based on instantaneous travel time/cost information gained through broadcasting (Wie et al. 1990, Lam and Huang 1995, Boyce et al. 1995, Li et al. 2000, Huang et al. 2009, Jiang et al. 2009, Friesz et al. 2010), and the predictive dynamic user-optimal (PDUO) assignment, in which an individual chooses a route that minimizes his/her actual travel time/cost based on predictive travel time/cost information gained through experience (Tong and Wong 2000, Hoogendoorn and Bovy 2004, Du et al. 2013). In DSO models, each user is assigned the route that minimizes the total travel time/cost of the system (Ghali and Smith 1995, Ziliaskopoulos 2000, Clarka et al. 2009, Carey and Watling 2012, Tao et al. 2014).

Conceptually, there are two common modeling approaches to traffic equilibrium problems: the discrete (or microscopic) modeling approach and the continuum (or macroscopic) modeling approach (Jiang et al. 2011). The discrete modeling approach, in which each road link within the network is modeled separately and demand is assumed to be concentrated at hypothetical zone centroids, is used for detailed studies of travel patterns in road network systems. Discrete DTA models are used in mathematical programs (Ziliaskopoulos 2000, Carey and Watling 2012), optimal control theory (Wie et al. 1990, Lam and Huang 1995), studies of variational inequality (Li et al. 2000, Friesz et al. 2010), and computer simulations (Yang et al. 1993, Fukui and Ishibashi 2010). Based on the reasonable assumption that travelers make certain behavioral choices, these discrete models can effectively represent the time-dependent nature of traffic demand and flow in transportation systems. However, it is both challenging and demanding to model a large-scale congested urban traffic network with a large number of links, intersections, interchanges, and severe congestion with queues and spillbacks. Furthermore, some of the what-if questions asked during the initial or conceptual phase of studies of such complex systems do not require very detailed results.

Due to its various advantages, the continuum modeling approach has recently been used in regional studies and for modeling highly dense transportation systems. In the continuum approach, a dense network is approximated as a continuum on which travelers are free to choose their paths in a two-dimensional (2D) continuous space. In this modeling approach, the characteristics of a network, such as its flow intensity, demand, and travel cost, can be represented by smooth mathematical functions and therefore less data are required for the model setup process. Furthermore, this approach can reduce the problem size (which depends on the method adopted to approximate the modeling region rather than on the actual number of links modeled) for a large/dense transportation network and thus save on computational time and memory. Early studies used static continuum equilibrium models to determine facility locations and perform policy, environmental, and socio-economic analyses (e.g., Wong (1998), Yang and Wong (2000), Daniele et al. (2003), Ho et al. (2006), Yin et al. (2013), Ho et al. (2013)). These static models might be adequate for the long-term prediction of network planning, design, and routing, but have limitations for short-term traffic predictions. Therefore, to investigate the macroscopic features and route choice behavior of travelers, continuum static user-optimal models have been extended to continuum DTA models for pedestrian flow (Xia et al. 2008, Huang et al. 2009, Jiang et al. 2009, 2012) and urban traffic flow (Rossa et al. 2010, Jiang et al. 2011, Du et al. 2013, Saumtally et al. 2013).

The modeling and simulation of real urban networks are complicated by problems such as heterogeneous users, elastic travel demands, and multi-modal networks, which have important effects on traffic performance. Both the accuracy and the explanatory ability of DTA models can be improved significantly by distinguishing classes of drivers and their specific driving characteristics (Hoogendoorn and Bovy 2000). The heterogeneous users of a traffic flow in a transportation system can be classified according to their reasons for traveling, vehicle types, and consumption values, etc. Each class is then modeled as an equilibrium. Static multiclass user equilibrium models (Wong 1998, Ho et al. 2006, 2013) have been generalized to bi-direction pedestrian flow models that satisfy the reactive continuum DUO principles (Jiang et al. 2009, 2012). Traffic demand and flow patterns in real-world urban road systems are influenced by a variety of parameters in the demand functions, and demand may be adversely affected by traveltime/cost (Babonneau and Vial 2008). Traffic demand reflects more realistic travel behavior, as travelers can change their trip frequency, departure time, transportation mode, and so on to avoid traffic congestion and tolls. For example, as congestion increases, travelers may decide to use a different mode of travel (e.g. an underground transport system that does not interfere with the road system), shift their time of travel (outside the design period), or forgo some trips altogether (Xu and Gao 2007).

Elastic demand models, in which the number of trips between each origin-destination (O-D) pair varies with the network conditions, consider user responses to changes in network costs in an aggregate way, different from re-routing. In reactive/predictive DTA models with elastic demand, whether reactive types such as those in Wie (1991), Yang (1997), Xu and Gao (2007), Ryu et al. (2014), or predictive types such as those in Szeto and Lo (2004), Han et al. (2011), Friesz and Meimand (2014), the travel demand is generally assumed to be a monotonically decreasing function with respect to the instantaneous/actual minimum travel time/cost between each OD pair. The inclusion of multiple user classes and the consideration of elastic demand can refine the framework of equilibrium DTA models. In fact, there are many discrete DTA models with multiple user classes and elastic demand in the literature (Cantarella 1997, Nagurney and Dong 2002, Clarka et al. 2009, Han et al. 2011, Xu et al. 2014), but few are continuum DTA models.

In this study we develop a macroscopic DTA model with elastic demand for a polycentric urban city with multiple compact central business districts (CBDs). The model is characterized by continuous independent variables and is expected to investigate the macroscopic characteristics and route choice behavior of multiple copies of urban traffic flow. A copy of flow is defined as the traffic movements heading to a CBD or a destination, as in Potts and Oliver (1972). For each copy of flow, the model is formulated as a flow conservation equation coupled with an Eikonal-type equation to describe the traffic flow propagation and assignment patterns, respectively. We postulate that travelers' path choice decisions are based on radio broadcasting information or route guidance system information that is provided on a real-time basis at the time of decision-making. Each copy of flow can follow the reactive continuum DUO principle by making strategic path choices to minimize the travel cost between the departure point and destination location. The traffic demand is assumed to be influenced by the level of service on the network, and thus for each copy of flow, the instantaneous traffic demand depends on the instantaneous total travel cost. We also derive the hyperbolicity of the continuum DTA model with elastic demand. A solution algorithm for the model is presented based on a cell-centered finite volume spatial discretization method and a fast sweeping method on unstructured meshes. Our numerical examples are designed to verify the rationality of the model and the effectiveness of the numerical method.

The rest of the paper is organized as follows. Section 2 provides the mathematical formulation for the DTA model with elastic demand in a polycentric urban city. Section 3 describes a solution algorithm for the DTA model. In Section 4, numerical examples are presented to test the rationality of the model and the efficiency of the algorithm. General conclusions are presented in Section 5.

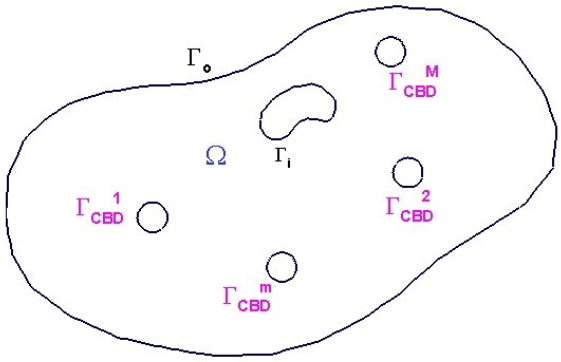

Figure 1 A polycentric urban region of arbitrary shape

2. Problem Formulation

Consider a polycentric urban region of arbitrary shape with $M(M \geq 2)$ compact CBDs (Figure 1). In the region, the road network is very dense and can be viewed as a 2D continuum. The urban region and its boundary are denoted by Ω (in km^2) and Γ (in km), respectively. Let Γ_o (in km) be the outer boundary of Ω, Γ_c^m (in km) be the boundary of the m-th ($m = 1, 2, ..., M$) compact CBD, Γ_i (in km) be the boundary of an obstruction, such as a lake, where traffic is not allowed to enter or leave, and $\mathbf{n}$ be the unit normal vector going out of the region.

It is assumed that heterogeneous travelers continuously distributed over space are characterized by their choice of trip destination. The m-th copy of traffic flow represents the travelers who are traveling to the m-th CBD within the urban region. A DTA model with elastic demand for a polycentric urban city is developed to investigate the macroscopic characteristics of urban traffic flow and the path-choice behavior of the heterogeneous travelers on a continuum network. In general, traffic demand is influenced by the level of service on the network and by travelers' willingness to take a faster route based on available travel time/cost information (which is instantaneous through broadcasting or predictive through experience). Here, we suppose that each copy of flow knows the current instantaneous traffic conditions in the transportation system during a trip. For each copy of flow, if the perceived travel time/cost is high, travelers may decide not to travel or to travel using a different mode (e.g., a subway); if the perceived travel time/cost is low, then more travelers may be willing to switch to road-based transport. The time-varying demand function (or demand distribution) $q^m(x, y, t)$ (in $veh/km^2/hr$), as a representation of the aggregate effect of all of the decisions in the m-th copy of traffic flow, is assumed to be sensitive to changes in travel cost and is represented by

$$q^m(x, y, t) = q^m(\Phi^m(x, y, t), t), \tag{1}$$

where $\Phi^m(x,y,t)$ (in \$) denotes the total instantaneous travel cost incurred by the m-th copy of flow traveling from origin $(x,y) \in \Omega$ to the m-th CBD at time t. Based on Eq. (1), $q^m(x,y,t)dxdy$ is the traffic demand from the sub-area at $(x,y) \in \Omega$ at time t to the m-th CBD for each copy of flow. Here, we consider the traffic demand for each copy of flow $q^m(x,y,t)$ to be a monotonically decreasing function of the total instantaneous travel cost $\Phi^m(x,y,t)$ incurred by the m-th copy of flow (Wong 1998, Han et al. 2011). In other words, as $\Phi^m(x,y,t)$ grows, $q^m(x,y,t)$ decreases, and vice versa.

2.1. Flow Conservation Equations

Our method of modeling urban traffic flow at the macroscopic level is based on the assumption that traffic streams as a whole are comparable to fluid particle flows, for which suitable balance or conservation laws can be written. Based on the theory of continuous medium mechanics, the traffic density, flow vector, and demand for each copy of flow should satisfy the following continuity equation.

$$\rho_t^m(x,y,t) + \nabla \cdot \mathbf{F}^m(x,y,t) = q^m(x,y,t), \tag{2}$$

which describes the conservation of the m-th copy of traffic flow in a topographically homogeneous sub-area at $(x,y) \in \Omega$ without entrances or exits at time t. Here, $\rho^m(x,y,t)$ (in veh/km^2) is the traffic density of the m-th copy of flow at location $(x,y) \in \Omega$ and time t. $\mathbf{F}^m = (f_1^m(x,y,t), f_2^m(x,y,t))$ (in $veh/km/hr$) is the flow vector, where f_1^m, f_2^m are the flow fluxes in the x- and y- directions, respectively.

The average speed $U^m(x,y,t)$ (in km/hr) of the m-th copy of flow is a function of the sum of all of the densities at location $(x,y) \in \Omega$ and time t, i.e.:

$$U^m(x,y,t) = U_f^m(x,y) exp(-\beta \rho^2(x,y,t)), \tag{3}$$

where $\rho(x,y,t) = \sum_{m=1}^{M} \rho^m(x,y,t)$ is the total density of urban traffic flow, $U_f^m(x,y)$ (in km/hr) represents the free flow speed of the vehicles at location (x,y), and β is a positive scalar that is influenced by the urban road area ratio and the geometrics of the free section. The magnitude of $\mathbf{F}^m(x,y,t)$ (in $veh/km/hr$) is defined as

$$\| \mathbf{F}^m(x,y,t) \| = \rho^m(x,y,t) U^m(x,y,t). \tag{4}$$

Based on Eqs. (3) and (4), the maximum flow intensity, $\mathbf{F}^m(x,y,t)$, for each copy of flow is achieved at critical density

$$\rho_c = \frac{1}{\sqrt{2M\beta}}, \tag{5}$$

which is calculated by $\frac{\partial \| \mathbf{F}^m \|}{\partial \rho^m} = 0, m = 1, 2, ...M$. When density $\rho^m(x,y,t) < \rho_c$, the m-th copy of flow is in a non-congested state; otherwise, it is in a congested state.

2.2. Path Choice Constraints

We assume that each copy of flow at location $(x, y) \in \Omega$ always selects the routes that minimize the total travel cost to the destination based on instantaneous traffic information from a radio broadcasting service or route guidance system provided on a real-time basis at the time of decision-making. Let $C^m(x, y, t)$ (in $\$/km$) represent the local generalized transportation cost per unit distance of travel incurred by the m-th copy of flow at location (x, y) and time t. We formulate the cost distribution, $C^m(x, y, t)$, for each copy of flow as the following general form in consideration of different scenarios.

$$C^m(x, y, t) = \kappa(\frac{1}{U^m(x, y, t)} + \pi^m(\tilde{\rho}(x, y, t))), \tag{6}$$

where $\tilde{\rho} := \{\rho^1(x, y, t), \rho^2(x, y, t), ..., \rho^M(x, y, t)\}$, and κ (in \$) denotes the value of time. In Eq. (6), the term $\frac{\kappa}{U^m(x,y,t)}$, as the major factor, represents the cost associated with travel time, and the term $\kappa\pi^m(\tilde{\rho}(x, y, t))$, as the minor factor, represents other associated costs such as a preference for avoiding high-density regions or reducing collision conflicts. These conflicts express the mutual effects of different types of travelers occupying a common space.

The functional form of travel cost $\Phi^m(x, y, t)$ for the m-th copy of flow can be written as

$$\Phi^m(x, y, t) = \Phi^m(x_c, y_c, t) + \min_p \int_p C^m(x, y, t)ds, \tag{7}$$

where p denotes any path from origin $(x, y) \in \Omega$ to destination $(x_c, y_c) \in \Gamma_c^m$, and $\Phi^m(x_c, y_c, t)$ expresses the cost incurred by entering the m-th CBD at time t. We can obtain the reactive DUO conditions as the equilibrated flow pattern in a polycentric urban network:

$$C^m(x, y, t)\frac{\mathbf{F}^m(x, y, t)}{\| \mathbf{F}^m(x, y, t) \|} + \nabla\Phi^m(x, y, t) = 0. \tag{8}$$

From Eq. (8), the total instantaneous travel cost $\Phi^m(x, y, t)$ of the m-th copy of flow from an origin $(x, y) \in \Omega$ to the m-th CBD satisfies the following Eikonal-type equation

$$\| \nabla\Phi^m(x, y, t) \| = C^m(x, y, t). \tag{9}$$

Similar to Jiang et al. (2009), Eq. (8) can be shown as follows.

For the m-th copy of flow travelling along any used path p from location $(x, y) \in \Omega$ to destination $(x_c, y_c) \in \Gamma_c^m$, the total instantaneous cost incurred by that copy of flow can be obtained by

$$\begin{aligned}\bar{C}_p^m(x, y, t) &= \int_p C^m(x, y, t)ds = \int_p C^m(x, y, t)\frac{\mathbf{F}^m(x, y, t)}{\| \mathbf{F}^m(x, y, t) \|} \cdot \mathbf{ds} \\ &= -\int_p \nabla\Phi^m(x, y, t) \cdot \mathbf{ds} = -(\Phi^m(x_c, y_c, t) - \Phi^m(x, y, t))\end{aligned}$$

$$= \Phi^m(x,y,t) - \Phi^m(x_c,y_c,t), \tag{10}$$

using Eqs. (8)-(9) and $\frac{\mathbf{F}^m(x,y,t)}{\|\mathbf{F}^m(x,y,t)\|}$, a unit vector that is parallel to **ds** along the path. The total instantaneous travel cost at time t is thus independent of the used paths.

In contrast, for an unused path $\tilde{p}$ between location $(x,y) \in \Omega$ and destination $(x_c,y_c) \in \Gamma_d^m$, the total travelling cost incurred by the m-th copy of flow is

$$\begin{aligned}\bar{C}_{\tilde{p}}^m(x,y,t) &= \int_{\tilde{p}} C^m(x,y,t)ds \geq \int_{\tilde{p}} C^m(x,y,t)\frac{\mathbf{F}^m(x,y,t)}{\| \mathbf{F}^m(x,y,t) \|} \cdot \mathbf{ds} \\ &= -\int_{\tilde{p}} \nabla\Phi^m(x,y,t) \cdot \mathbf{ds} = -(\Phi^m(x_c,y_c,t) - \Phi^m(x,y,t)) \\ &= \Phi^m(x,y,t) - \Phi^m(x_c,y_c,t),\end{aligned} \tag{11}$$

using Eqs. (8)-(9).

The inequality in (11) occurs because of some segments along path $\tilde{p}$ whose normal vectors $\frac{\mathbf{F}^m(x,y,t)}{\|\mathbf{F}^m(x,y,t)\|}$ are not parallel to **ds**: $ds > (\frac{\mathbf{F}^m(x,y,t)}{\|\mathbf{F}^m(x,y,t)\|}) \cdot \mathbf{ds}$ for the segments. For any unused paths, the total instantaneous travel cost is greater than or equal to that of the used paths. The model guarantees that each copy of flow chooses a path in the continuum road network in a user-optimal manner with respect to instantaneous travel information representing current traffic flow conditions.

A dynamic continuum model with elastic demand for a polycentric urban city can now be formulated as the following set of differential equations. The flow conservation equation for each copy of flow is

$$\begin{cases} \rho_t^m(x,y,t) + \nabla \cdot \mathbf{F}^m(x,y,t) = q^m(\Phi^m(x,y,t),t), \forall (x,y) \in \Omega, \\ \mathbf{F}^m(x,y,t) = -\frac{\rho^m(x,y,t)U^m(x,y,t)\nabla\Phi^m(x,y,t)}{C^m(x,y,t)}, \forall (x,y) \in \Omega, \\ \mathbf{F}^m(x,y,t) \cdot \mathbf{n} = 0, \forall (x,y) \in \Gamma \setminus \Gamma_c^m, \\ \rho^m(x,y,0) = \rho_0^m(x,y), \forall (x,y) \in \Omega, \end{cases} \tag{12}$$

which is coupled with the Eikonal-type equation

$$\begin{cases} \| \nabla\Phi^m(x,y,t) \| = C^m(x,y,t), \ \forall (x,y) \in \Omega, \\ \Phi^m(x,y,t) = \Phi_0^m(x,y,t), \ \forall (x,y) \in \Gamma_c^m, \end{cases} \tag{13}$$

where $\Phi_0^m(x,y,t)$ represents the cost incurred by entering the m-th CBD at time t and $m = 1,2,...,M$.

Note that although the dynamic continuum model (12) is reactive, the decision to travel or not to travel in each copy of flow is made at the beginning of the trip (e.g., at home). Once travelers have made the decision to travel, the next decision is the route choice. Thus, for each copy of flow, the demand is made at the beginning of an O-D pair, and does not change in the middle of a journey (as governed by the conservation law (2)).

2.3. Hyperbolicity of the Model

Let

$$\bar{\rho}=\begin{bmatrix}\rho^1\\ \rho^2\\ \vdots\\ \rho^m\\ \vdots\\ \rho^M\end{bmatrix},\quad \bar{f}_1=\begin{bmatrix}\rho^1U^1\nu_1^1\\ \rho^2U^2\nu_1^2\\ \vdots\\ \rho^mU^m\nu_1^m\\ \vdots\\ \rho^MU^M\nu_1^M\end{bmatrix},\quad \bar{f}_2=\begin{bmatrix}\rho^1U^1\nu_2^1\\ \rho^2U^2\nu_2^2\\ \vdots\\ \rho^mU^m\nu_2^m\\ \vdots\\ \rho^MU^M\nu_2^M\end{bmatrix},\quad \bar{q}=\begin{bmatrix}q^1\\ q^2\\ \vdots\\ q^m\\ \vdots\\ q^M\end{bmatrix},$$

where $\vec{\nu}^m=(\nu_1^m,\nu_2^m)$ is a unit vector in the direction of motion for the m-th copy of flow. Based on Eq. (4), $\mathbf{F}^m=\rho^mU^m\vec{\nu}^m$.

From Eq. (2), the flow conservation equations for M copies of urban traffic flow can be described as the following system.

$$\bar{\rho}_t+\nabla\cdot\bar{\mathbf{F}}=\bar{q}, \tag{14}$$

where $\bar{\mathbf{F}}=(\bar{f}_1,\bar{f}_2)$. Given that the travel direction of the m-th copy of flow $\vec{\nu}^m$ is predefined, the hyperbolicity of system (14) can be obtained.

The linearized form of (14) is

$$\bar{\rho}_t+A\bar{\rho}_x+B\bar{\rho}_y=\bar{q},$$

where flux Jacobian matrices A and B are respectively calculated by

$$A=\frac{\partial\bar{f}_1}{\partial\bar{\rho}}=(a_{ij}),\quad a_{ij}=U^i\nu_1^i\delta_{ij}+c_{ij},\quad c_{ij}=\rho^i\frac{\partial U^i}{\partial\rho^j}\nu_1^i,$$

$$B=\frac{\partial\bar{f}_2}{\partial\bar{\rho}}=(b_{ij}),\quad b_{ij}=U^i\nu_2^i\delta_{ij}+\tilde{c}_{ij},\quad \tilde{c}_{ij}=\rho^i\frac{\partial U^i}{\partial\rho^j}\nu_2^i.$$

Based on Eq. (3), we have

$$\frac{\partial U^m}{\partial\rho^1}=\frac{\partial U^m}{\partial\rho^2}=...=\frac{\partial U^m}{\partial\rho^m}=...=\frac{\partial U^m}{\partial\rho^M}=\frac{dU^m}{d\rho}.$$

The composite Jacobian matrix is defined as $F_n=An_x+Bn_y$, where (n_x,n_y) is a non-zero unit vector. The characteristic polynomial of F_n is

$$\begin{vmatrix}U^1\omega^1+c_1-\lambda & c_1 & \dots & c_1 & c_1\\ c_2 & U^2\omega^2+c_2-\lambda & \dots & c_2 & c_2\\ \vdots & \vdots & \ddots & \vdots & \vdots\\ c_{M-1} & c_{M-1} & \dots & U^{M-1}\omega^{M-1}+c_{M-1}-\lambda & c_{M-1}\\ c_M & c_M & \dots & c_M & U^M\omega^M+c_M-\lambda\end{vmatrix},$$

where $\omega^m=\nu_1^mn_x+\nu_2^mn_y$ and $c_m=\rho^m\omega^m\frac{dU^m}{d\rho}$, $1\le m\le M$.

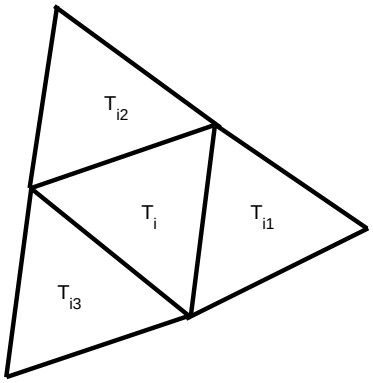

Figure 2 A typical unstructured triangular grid.

Subtracting Column $i-1$ from Column i $(i=M,...,2)$ of the determinant described above gives us,

$$\begin{vmatrix} U^1\omega^1+c_1-\lambda & \lambda-U^1\omega^1 & \dots & 0 & 0 \\ c_2 & U^2\omega^2-\lambda & \dots & 0 & 0 \\ \vdots & \vdots & \ddots & \vdots & \vdots \\ c_{M-1} & 0 & \dots & U^{M-1}\omega^{M-1}-\lambda & \lambda-U^{M-1}\omega^{M-1} \\ c_M & 0 & \dots & 0 & U^M\omega^M-\lambda \end{vmatrix} := P_M(\lambda).$$

From Zhang et al. (2006), we know that characteristic polynomial $P_M(\lambda)$ has M unequal real roots, and system (14) is therefore strictly hyperbolic.

3. Solution Procedure

To solve the dynamic continuum model composed of Eqs. (12) and (13), the cell-centered finite volume spatial discretization method for the flow conservation equation in Eq. (12) and the fast sweeping method for the Eikonal-type equation in Eq. (13) on unstructured triangular meshes are introduced. Let $\mathcal{T}^h := \bigcup_{T_i\in\mathcal{T}^h} T_i$ be a regular triangulation of the computational domain Ω with N_p nodes, N_t cells, and N_f faces. The size of the discretization is defined by $h := super_{T_i\in\mathcal{T}^h}\{h_{T_i}\}$, where h_{T_i} is the exterior diameter of the triangular cell T_i. The neighboring triangles of T_i are denoted T_{ik} with a counter-clockwise convention, as sketched in Figure 2.

3.1. Finite Volume Spatial Discretization

In this subsection, the total instantaneous travel cost $\Phi^m(x,y,t)$ for each copy of flow is assumed to be known for all $(x,y)\in\Omega$ and time t. The cell-centered finite volume method is considered: each triangular cell T_i represents a control volume. The unknowns, which are the densities of the m-th copy of flow, are stored in the geometric centers of the cells.

Integrating Eq. (12) over each control volume T_i and using the Gauss theorem yields

$$\frac{\partial\rho^m(x_i,y_i,t)}{\partial t}+\frac{1}{A_i}\oint_{\partial T_i}\mathbf{F}^m(x,y,t)\cdot\mathbf{n}_i ds = q^m(\Phi^m(x_i,y_i,t),t), \tag{15}$$

where (x_i, y_i), A_i, ∂T_i, and $\mathbf{n}_i$ are the geometric center, area, boundary, and outward unit normal vector of the triangular cell T_i respectively. The integral expression $\oint_{\partial T_i} \mathbf{F}^m(x,y,t) \cdot \mathbf{n}_i ds$ in Eq. (15) is approximately calculated by

$$\oint_{\partial T_i} \mathbf{F}^m \cdot \mathbf{n}_i ds = \sum_{k=1}^{3} \left(\tilde{\mathbf{F}}^m \cdot \mathbf{n}\right)_{ik} |l_{ik}|, \tag{16}$$

where $|l_{ik}|$ is the length of the k-th edge l_{ik} of T_i, $\mathbf{n}_{ik}$ represents the corresponding unit normal vector going out of T_i, and $\tilde{\mathbf{F}}^m_{ik}$ denotes the numerical flux through the middle point of l_{ik}, $k = 1, 2, 3$. See Jiang et al. (2009) for details of the numerical method used to calculate the numerical flux $\tilde{\mathbf{F}}^m_{ik}$.

3.2. Calculation of $\nabla\Phi^m$ on the Control Volume Surfaces

In this subsection, we assume that the traffic density $\rho^m(x,y,t)$ for each copy of flow is known for all $(x,y) \in \Omega$ and time t. On each triangular cell T_i the total instantaneous travel cost $\Phi^m(x,y,t)$ for each copy of flow is approximated by the following linear function:

$$\Phi^m(x,y,t)|_{T_i} = \sum_{k=1}^{3} \hat{N}_k \Phi^m_k,$$

Its gradient on T_i is thus approximated by a constant vector,

$$\nabla\Phi^m(x,y,t)|_{T_i} = \sum_{k=1}^{3} \nabla\hat{N}_k \Phi^m_k, \tag{17}$$

where $\{\hat{N}_k\}_{k=1}^3$ is the set of Lagrangian interpolation bases and $\Phi^m_k, k = 1, 2, 3$ are the values of Φ^m at the three vertices of the triangular cell T_i. For each copy of flow, the values of Φ^m at all of the grid points can be solved by the fast sweeping method based on Eq. (13). Further details of this procedure are described in Xia et al. (2008) and Qian et al. (2007)).

3.3. Time Discretization

A second-order explicit total variation diminishing Runge-Kutta time-stepping method (Shu and Osher 1988) is chosen to discretize Eq. (15) and thus the coupled system composed of Eqs. (12) and (13) can be decoupled. Note that the flux vector $\mathbf{F}^m$ in Eq. (12) is relevant to the value of $\nabla\Phi^m$. Therefore, at each time step we must first obtain the values of $\nabla\Phi^m$ at all of the grid points of the unstructured triangular meshes based on the known value of $\{(\rho^m)^n\}$ at the n-th time step (see Subsection 3.2). The solution value of $\{(\rho^m)^{n+1}\}$ at the $(n+1)$-th time step can then be obtained from $\{(\rho^m)^n\}$ at the n-th time step as follows.

$$(\rho^m)_i^{(1)} = (\rho^m)_i^n - \frac{\Delta t}{A_i} \sum_{k=1}^{3} (\tilde{\mathbf{F}}^m \cdot \mathbf{n})_{ik}^n |l_{ik}| + \Delta t (q^m)_i^n, \tag{18}$$

$$(\rho^m)_i^{n+1} = \frac{1}{2}[(\rho^m)_i^n + (\rho^m)_i^{(1)} - \frac{\Delta t}{A_i}\sum_{k=1}^{3}(\tilde{\mathbf{F}}^m \cdot \mathbf{n})_{ik}^{(1)}|l_{ik}| + \Delta t(q^m)_i^{(1)}], \tag{19}$$

where the choice of the time step Δt must satisfy the Courant-Friedrichs-Lewy condition and $m = 1, 2, ..., M$.

4. Numerical Experiments

In this section, a numerical example is designed to verify the rationality of the developed dynamic continuum model with elastic demand for a polycentric urban city and the validity of the numerical method of the model. Consider a model city (see Figure 1) with two compact CBDs, CBD 1 and CBD 2, located at $(14\ km, 20\ km)$ and $(31\ km, 23\ km)$, respectively, both with a diameter of $1\ km$. The users traveling to CBD 1 and CBD 2 are called Copy 1 and Copy 2, respectively. The modeling period is 6:00 am-11:00 am, i.e. $t \in T = [0\ hr, 5\ hr]$.

The elastic traffic demand function $q^m(\Phi^m(x, y, t), t)$ for each copy of flow is assumed to be

$$q^m(\Phi^m(x, y, t), t) = q_{max}^m[1 - \gamma_1\Phi^m(x, y, t)]g^m(t), m = 1, 2, \tag{20}$$

where q_{max}^m (in $veh/km^2/hr$) is the maximum demand of each copy of flow and γ_1 is a positive scalar taking $0.002\ \$^{-1}$. In Eq. (20), the factor $[1-\gamma_1\Phi^m(x, y, t)]$ accounts for the greater number of trips that will be generated in the domain with lower cost, which explains that the traffic demand is elastic. The function $g^m(t)$ represents the periodically changing nature of the demand. Here, $g^1(t)$ is defined by

$$g^1(t) = \begin{cases} t/2, & t \in [0\ hr, 2\ hr], \\ 2 - t/2, & t \in [2\ hr, 4\ hr], \\ 0, & t \in [4\ hr, 5\ hr], \end{cases}$$

and $g^2(t)$ is defined by

$$g^2(t) = \begin{cases} t, & t \in [0\ hr, 1\ hr], \\ 1, & t \in [1\ hr, 3\ hr], \\ 4 - t, & t \in [3\ hr, 4\ hr], \\ 0, & t \in [4\ hr, 5\ hr]. \end{cases}$$

In Eq. (3), the parameter β is set to 2×10^{-6} and the free-flow speed function $U_f^m(x, y)$ is given by

$$U_f^m(x, y) = U_{max}^m[1 + \gamma_2 d^m(x, y)],$$

where U_{max}^m is the maximum speed of each copy of flow, $d^m(x, y)$ is the distance between a location $(x, y) \in \Omega$ and the center of the m-th CBD, and $\gamma_2 = 0.004\ km^{-1}$. Based on Eq. (5), the critical

density ρ_c, which is characterized by the coexistence of the free flow traffic and jammed traffic phases in the modeling domain, is $\rho_c \approx 353.55 veh/km^2$. In Eq. (6), $\kappa = 75$ \$/hr and

$$\pi^1(\tilde{\rho}(x,y,t)) = \pi_0[\frac{\rho^2(x,y,t)}{\rho^1(x,y,t)+\rho^2(x,y,t)}]^2, \tag{21}$$

$$\pi^2(\tilde{\rho}(x,y,t)) = \pi_0[\frac{\rho^1(x,y,t)}{\rho^1(x,y,t)+\rho^2(x,y,t)}]^2, \tag{22}$$

with $\pi_0 = 0.0025$ hr/km. Eqs. (21) and (22) represent the extra expense incurred by the collision avoidance behavior of two types of travelers during their encounter in the common space.

It is assumed that there is no traffic at the beginning of the modeling period, i.e., $\rho_0^m(x,y) = 0, \forall (x,y) \in \Omega$, and that no cost is incurred on entering each CBD, i.e., $\Phi_0^m(x,y,t) = 0, \forall (x,y) \in \Gamma_c^m, t \in T$. For the m-th copy of flow, the total load demand $q_\Omega^m(t)$ over the whole domain at time t, and the corresponding cumulative demand $Q_\Omega^m(t)$ are calculated respectively by

$$q_\Omega^m(t) = \int_t \int_\Omega q^m(\Phi^m(x,y,t),t)dxdy,$$
$$Q_\Omega^m(t) = \int_0^t q_\Omega^m(\xi)d\xi,$$

The total inflow $f_{CBD}^m(t)$ through Γ_c^m at time t, and the corresponding cumulative inflow $F_{CBD}^m(t)$ are expressed by

$$f_{CBD}^m(t) = \oint_{\Gamma_c^m} (\mathbf{F}^m \cdot \mathbf{n})(x,y,t)ds,$$
$$F_{CBD}^m(t) = \int_0^t f_{CBD}^m(\xi)d\xi.$$

Scenarios	Copy 1		Copy 2	
	q_{max}^1	u_{max}^1	q_{max}^2	u_{max}^2
Scenario 1	400	65	300	65
Scenario 2	300	65	400	65
Scenario 3	400	80	300	80
Scenario 4	300	80	400	80
Scenario 5	300	80	400	65
Scenario 6	300	65	400	80

Table 1 Simulated scenarios with different model parameters.

We now investigate the effects of the model parameters on the macroscopic characteristics of urban traffic flow, such as the density distributions and route choice behavior of multiple copies of urban traffic flow. We consider several scenarios and vary the model parameter values, such as the peak value of traffic demand and travel speed, for each copy of flow (see Table 1). To verify the convergence of the numerical method for the proposed model, we test three different meshes

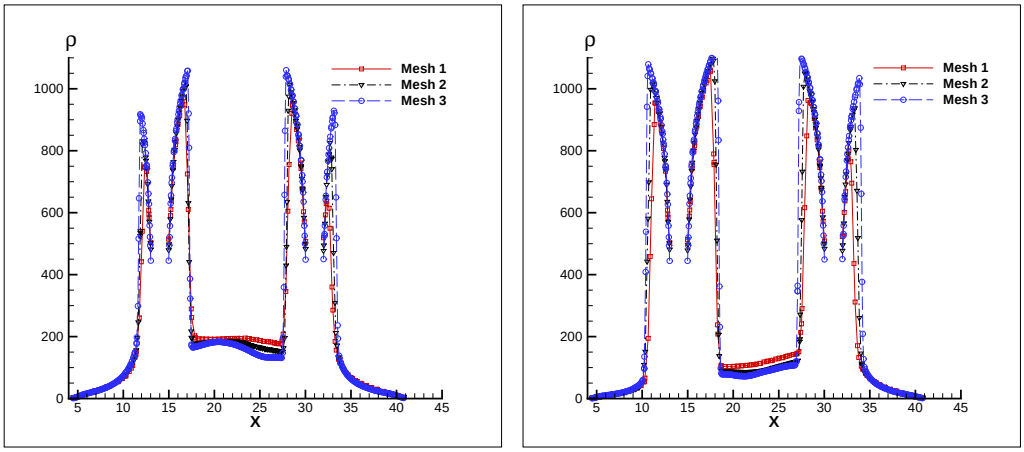

(a)$t = 2hr$ (b)$t = 3hr$

Figure 3 **The plot of the total density ρ.**

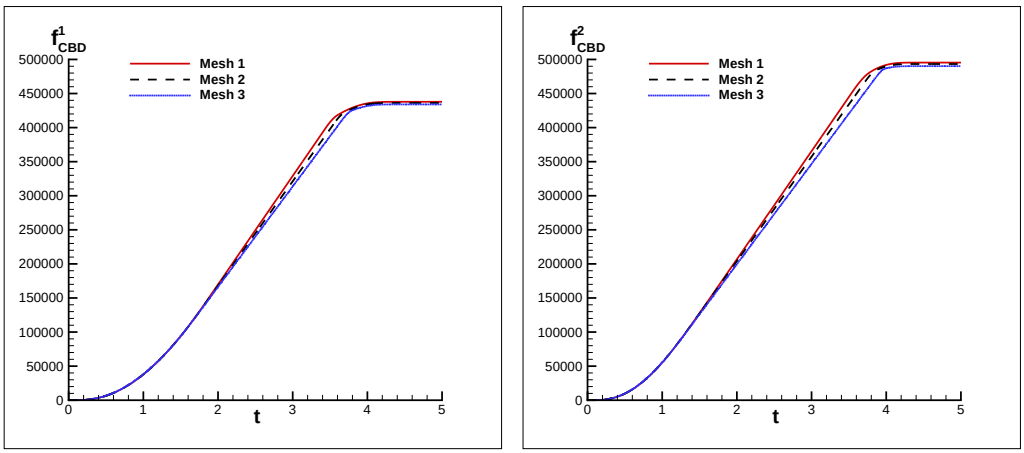

(a)$F^1_{CBD}(t)$ (b)$F^2_{CBD}(t)$

Figure 4 **The plot of the cumulative inflow $F^m_{CBD}(t)$.**

of triangular elements (Mesh 1: 2,464 nodes and 4,731 elements; Mesh 2: 5,614 nodes and 10,919 elements; Mesh 3: 22,653 nodes and 44,661 elements) in Scenario 1. Figure 3 shows the curves of total density ρ along the line passing through the centers of two CBDs, i.e., (14 km, 20 km) and (31 km, 23 km), at different times. Shocks are clearly seen around both CBDs due to the increasing number of travelers gathering around them and their limited capacity. In addition, traffic congestion occurs when the two copies of flow queue up to enter the CBDs. Figure 4 plots the cumulative inflow, $F^m_{CBD}(t)$, for each copy of flow. It can be seen from both Figures 3 and 4 that the curves for Meshes 1, 2, and 3 in each sub-figure nearly coincide, which indicates the good convergence behavior of the model's numerical algorithm.

The following numerical experiments are performed on an unstructured triangular grid with 3,266 nodes and 6,298 elements (see Figure 5).Figure 6 shows the density distributions for the dissipation

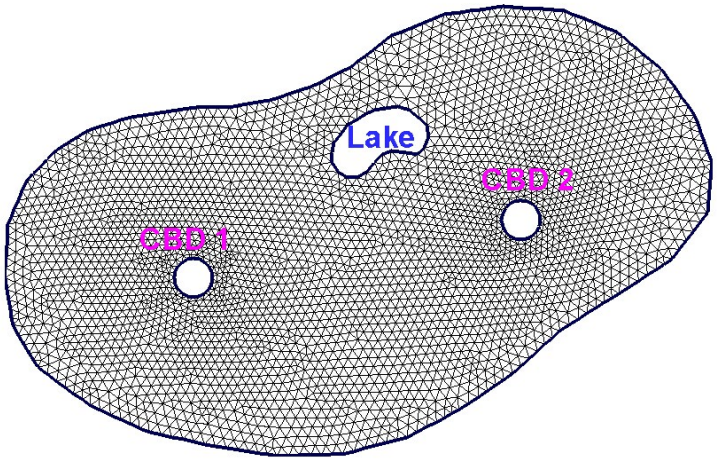

Figure 5 The unstructured triangular grid.

of two copies of urban traffic flow in four phases in Scenario 1. In the first phase ($t = 1hr$), Copy 1 displays almost a free-flow state and does not appear near CBD 2, whereas Copy 2 has light traffic congestion (i.e., the flow density exceeds the critical density, $\rho_c \approx 353.55veh/km^2$) within a narrow range of the western regions of CBD 2. To avoid collision conflict with Copy 1, Copy 2 tries to travel away from CBD 1. In the second phase ($t = 2hr$), as more travelers gather around their destinations and wait in line for entry to the CBDs during rush hours in both copies, traffic jams are caused within about 2 kilometres of each CBD. Copy 1's density is higher in the eastern part of CBD 1's boundary as the location of CBD 1 within the domain causes more traffic to arrive from the east of the model city. The opposite phenomenon is observed for Copy 2. To reduce the total travel cost, travelers in each copy of flow may drive close to each other's destination at the peak times, although there exists a risk of collision. In the third phase ($t = 3hr$), despite lower demand, the traffic jams spread to a wider range of nearby areas of the two CBDs, as the arriving travelers pile up on the road network. In the fourth phase ($t = 4hr$), the travelers gathered around the two CBDs travel to their own destinations and each copy of flow recovers to the free-flow state.

Figure 7 depicts the density distributions for the dissipation of two copies of urban traffic flow in four phases in Scenario 2. In the first phase ($t = 1hr$), the spatial distribution of the density ρ^2 is slightly different from Figure 6 (b) and the congested region is wider (see Figure 7 (b)). In the second phase ($t = 2hr$), light traffic congestion occurs in the eastern part of CBD 1's boundary. In contrast, heavy traffic congestion emerges in Copy 2 and spreads within several kilometers of the surrounding regions of CBD 2, due to greater traffic demand loading onto the network during rush hour. The heavy congestion expands to the south-east border of the city, which is close to the southern part of CBD 2's boundary. In the third phase ($t = 3hr$), traffic congestion propagates

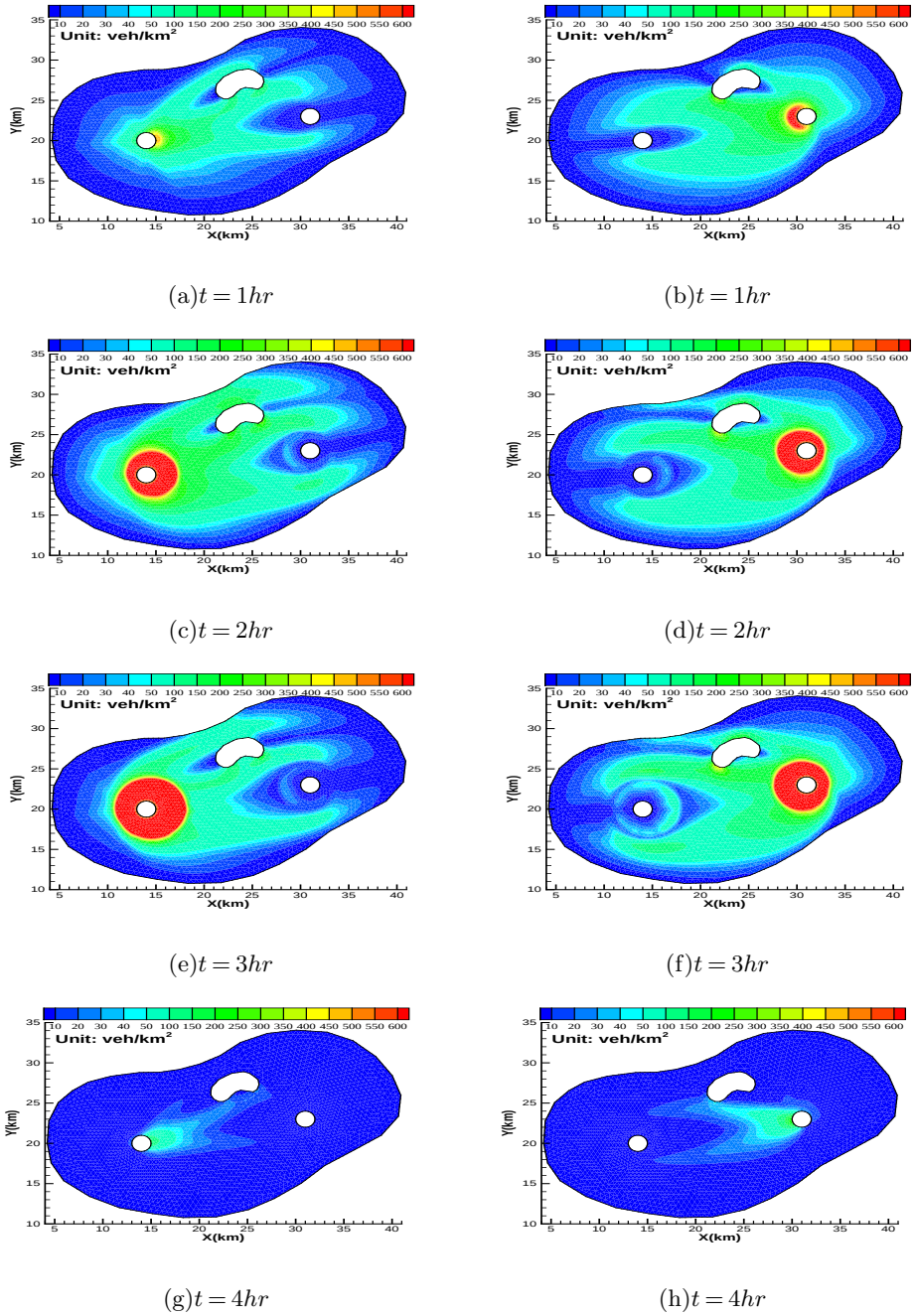

(a)$t = 1hr$ (b)$t = 1hr$

(c)$t = 2hr$ (d)$t = 2hr$

(e)$t = 3hr$ (f)$t = 3hr$

(g)$t = 4hr$ (h)$t = 4hr$

Figure 6 Density plot of Scenario 1 (left: Copy 1; right: Copy 2).

very rapidly through the middle ground (across the lake) between the two CBDs. More serious congestion is observed in Copy 2 as more travelers gather on the roads around CBD 2 and queue up for entry into CBD 2 (see Figure 7 (f)). The resulting traffic flow in Copy 1 is in the free-flow state around CBD 1 and the congested region is much closer to CBD 2 (see Figure 7 (e)). Copy 2 is the major stream on the network as it has a greater loaded traffic demand. The minor stream, Copy 1, will give way to the major stream, if the two copies of flow interact in the common area.

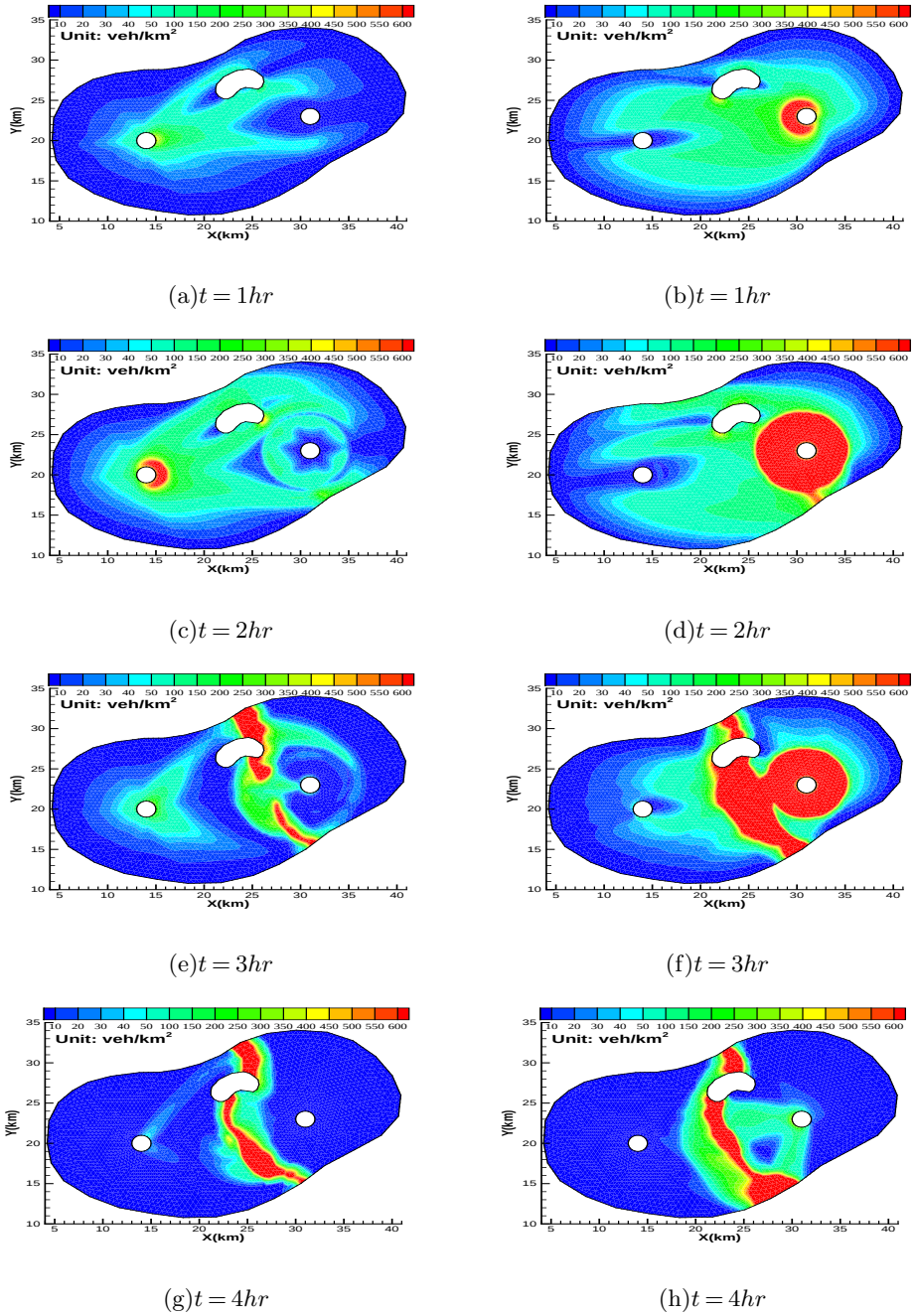

(a)$t = 1hr$ (b)$t = 1hr$

(c)$t = 2hr$ (d)$t = 2hr$

(e)$t = 3hr$ (f)$t = 3hr$

(g)$t = 4hr$ (h)$t = 4hr$

Figure 7 Density plot of Scenario 2 (left: Copy 1; right: Copy 2).

This can explain a typical self-organization phenomenon observed in urban transportation systems. In the fourth phase ($t = 4hr$), traffic congestion continues, but the crowded conditions in Copy 2 are alleviated.

Figure 8 shows the flow vector $\mathbf{F}^m(x, y, t)$ of each copy of flow at different times in Scenarios 1 and 2, to improve our understanding of the distribution and evolution of the two copies of urban traffic flow on the road networks. In Scenario 1, traffic congestion only occurs in the surrounding

area of each CBD (see Figure 8 (a), (c) and (e)) and quickly disappears as the reduced demand is reduced (see Figure 8 (g)). In Scenario 2, severe congestion appears around CBD 2 in the early stages (see Figure 8 (b) and (d)) and rapidly propagates to the regions far away from CBD 2 as the demand increases. Some of the roads used by Copy 1 traveling from the east of the city are thus blocked. As more vehicles assemble on the road network, two opposing '"strips", one Copy 1 and the other Copy 2, develop between the two CBDs (see Figure 8 (f) and (h)). This situation is similar to what we previously observed in crossing pedestrian flows (Hoogendoorn and Daamen 2005; Jiang et al. 2009), which demonstrates that this self-organization phenomenon also occurs for multiple copies of urban traffic flow. Over time, the over-crowded condition in the major stream of Copy 2 is alleviated first.

By comparing Scenarios 1 and 2 above, we observe that different maximum values of the traffic demand and travel speed for each copy of flow produce different traffic conditions in the continuum network Ω. In Figure 9, for each copy of flow, the total demand $q_\Omega^m(t)$ over the whole domain and the total inflow $f_{CBD}^m(t)$ through Γ_c^m are plotted for the two scenarios. In Scenario 1 (see Figure 9 (a)), for each copy of flow, $q_\Omega^m(t)$ and $g^m(t)$ change similarly over time, which indicates the periodically changing nature of demand. The available capacities of the two CBDs are very similar. Due to the long peak period (i.e., $t \in [1hr, 3hr]$) the inflow of CBD 2 reaches its maximum first and sustains it for more than two and a half hours, resulting in traffic congestion and delays. However, at $t = 4hr$, the road congestion improves as there is no traffic demand loaded into the road system. All of the travelers in each copy of flow can enter their respective CBDs during the modeled period. After $t = 4.5hr$ or so, there is no traffic on the road network. In Scenario 2 (see Figure 9 (b)), there are dramatic fluctuations in the $q_\Omega^m(t)$ and $f_{CBD}^m(t)$ curves for each copy of flow. This phenomenon occurs at a non-peak time (after $t = 2hr$) for Copy 1, but occurs during rush hour for Copy 2. The inflow of CBD 2 reaches its maximum when traffic congestion appears. For Copy 2, $q_\Omega^2(t)$ reaches its maximum at $t = 1hr$, then decreases until reaching zero at $t = 4hr$, which is different from the behavior of $g^2(t)$. The elastic change of the traffic demand and the total instantaneous travel cost $\Phi^1(x, y, t)$ explain this difference. When the road system is overcrowded for a long period, $\Phi^m(x, y, t)$ for each copy of flow increases significantly, which causes a drop in the demand. If we also consider the results in Figure 7, then we predict that the over-crowded status will continue until next modeling period, as $f_{CBD}^m(t)$ for each copy of flow does not decrease to zero at the end of this modeling period.

The corresponding cumulative demand $Q_\Omega^m(t)$ and the cumulative inflow $F_{CBD}^m(t)$ for each copy of flow are plotted in Figure 10. In Scenario 1 (see Figure 10 (a)), for each copy of flow there is

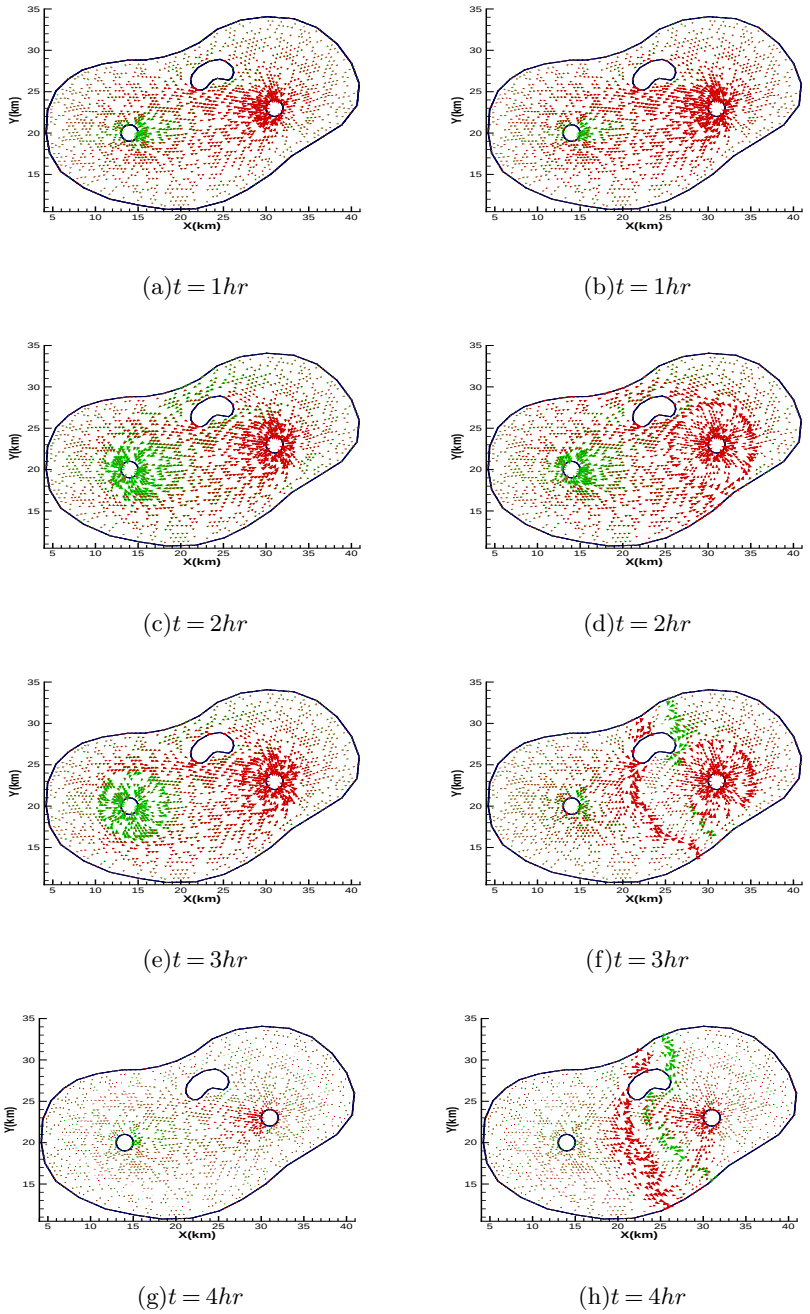

(a)$t = 1hr$ (b)$t = 1hr$

(c)$t = 2hr$ (d)$t = 2hr$

(e)$t = 3hr$ (f)$t = 3hr$

(g)$t = 4hr$ (h)$t = 4hr$

Figure 8 Flow vector plot (left: Scenario 1; right: Scenario 2; green: Copy 1; red: Copy 2).

a deviation between the $Q^m_\Omega(t)$ and $F^m_{CBD}(t)$ curves, at some point, which implies a traffic delay. However, the two curves coincide perfectly with each other at a certain point demonstrating that no traffic is detained in the system during the modeled period. In Scenario 2 (see Figure 10 (b)), the deviation between the two curves is much greater than in Figure 10 (a), which means more serious congestion. The two curves for each copy of flow also do not overlap until the end of the modeling period, which further shows that the traffic delay caused by traffic congestion will last

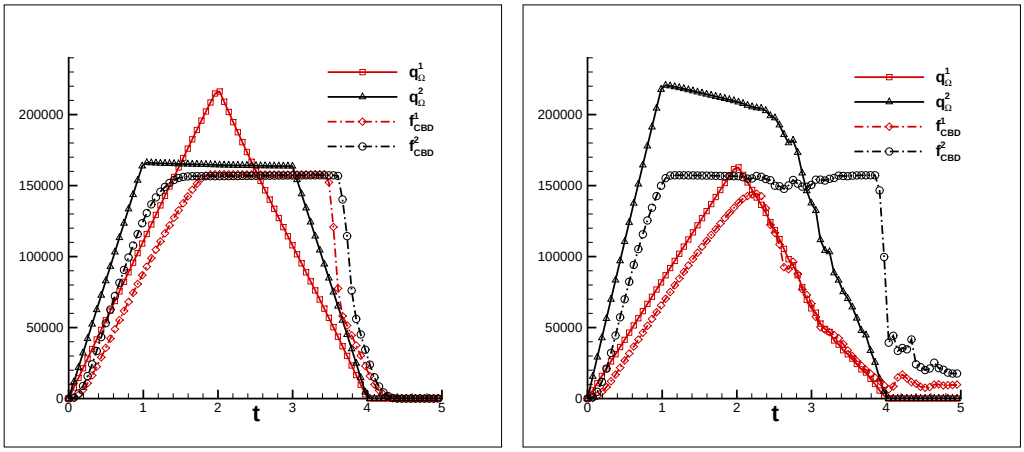

(a)Scenario 1 (b)Scenario 2

Figure 9 The total demand and total inflow of the two scenarios.

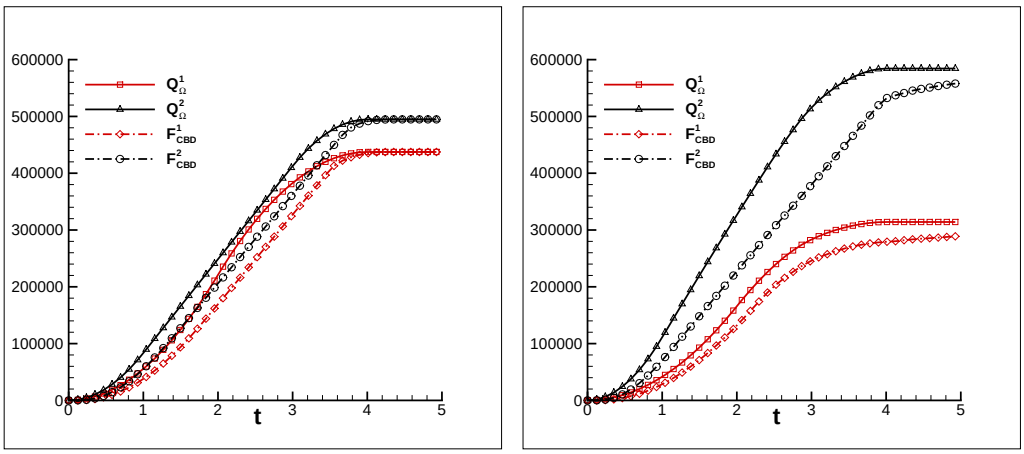

(a)Scenario 1 (b)Scenario 2

Figure 10 The cumulative demand and cumulative inflow of the two scenarios.

until the next modeling period.

Figure 11 illustrates how $f^m_{CBD}(t)$ changes across six scenarios. In Figure 11 (a), the two curves in Scenarios 4 and 6 almost coincide. Scenario 3 has the largest CBD 1 available capacity and Scenario 2 has the smallest. In Scenarios 1,3,4 and 6, $f^1_{CBD}(t)$ falls to zero, indicating that all of Copy 1 enter CBD 1. In Scenarios 2 and 5, there is an apparent fluctuation in the curves after $t = 2hr$, which demonstrates that a serious traffic jam occurs in the network and that part of Copy 1 will be stranded in these two scenarios. Similar results are observed in Figure 11 (b). For example, Scenarios 2 and 5 show the fluctuations in the $f^2_{CBD}(t)$ curve, showing that part of Copy 2 will be also stranded. The numerical results of these simulations suggest measures to ease urban traffic congestion from the macroscopic point of view. For example, some of the traffic demand of Copy 2 can be distributed to Copy 1 and/or the city's transportation infrastructure can be improved to

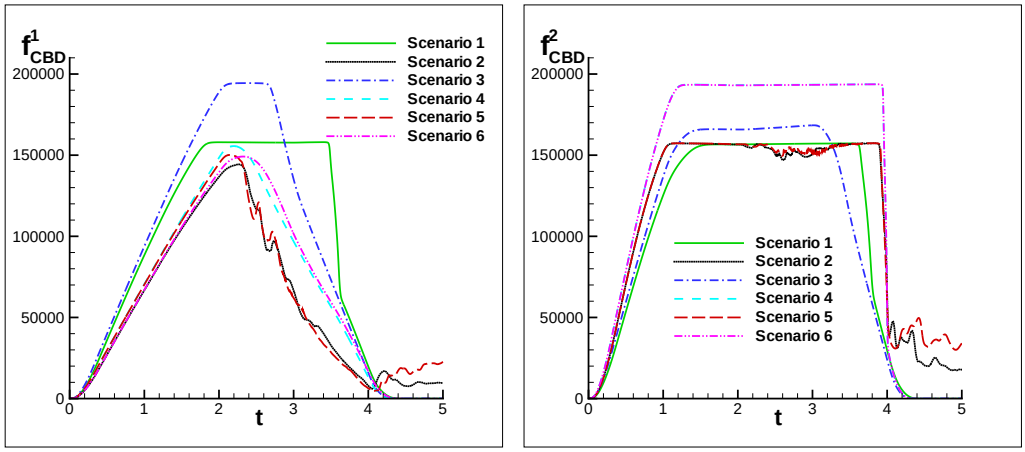

(a)$f^1_{CBD}(t)$ (b)$f^2_{CBD}(t)$

Figure 11 The total inflow of the six scenarios.

increase the maximum permissible user speed.

5. Conclusion

In this paper, we develop a dynamic traffic assignment model with elastic demand for a polycentric urban area that predicts the evolution of multiple copies of urban traffic flow over space and time in continuum time-varying transportation systems. The model satisfies the reactive dynamic user equilibrium principle, which describes the route choice behavior of each copy of flow. The model's numerical algorithm combines the cell-centered finite volume spatial discretization method and fast sweeping method on unstructured meshes. The results of numerical simulation show that the model is capable of investigating the macroscopic characteristics of multiple copies of urban traffic flow, such as the spatial distribution and temporal evolution of the flow densities and fluxes, and path choice behavior in response to elastic demand for each copy of flow. Our proposed model also captures observed traffic flow phenomena, such as self-organization and the building, propagation, and dissipation of congestion. We recommend macro-level measures for easing existing or avoiding future traffic congestion in polycentric urban areas.

The continuum or macroscopic modeling approach requires fewer data for the model setup process than the discrete or microscopic modeling approach, which requires detailed data for all road links and intersections included. The former is therefore particularly useful for highly populated urban regions such as the cities of many Asian countries, in which both population and road density are very high, and the attributes of roads and signalized intersections are rarely available. The better understanding of the global characteristics of a road network conferred by the model developed herein allows traffic control and management to be visualized and the qualitative diagnosis and

localization of traffic congestion to be improved. In this paper, we assume the travelers in a dense urban transportation system to be divided into two types based on their travel purpose and that each traveler type makes route choice in a reactive manner based on the desire to minimize their total instantaneous travel cost from origin to destination, i.e., to the select CBD. In follow-up work, we will consider the influence of consumption values, i.e., assume that different types of travelers place different values on time.

Acknowledgments

This work was jointly supported by the Research Foundation of SWUST (No. 10zx7137) and grants from the National Natural Science Foundation of China (Nos. 11202175, 11272199 and 11372294), the Research Grants Council of the Hong Kong Special Administrative Region of China (Project Nos. 717512, 17208614), the National Basic Research Program of China (No. 2012CB725404), and the National Research Foundation of Korea funded by the Korean Government (MEST) (No. NRF-2010-0029446).

References

Babonneau, F., J. P. Vial. 2008. An efficient method to compute traffic assignment problems with elastic demands. *Transport. Sci.* **42** 249–260.

Balijepalli, N. C., D. Ngoduy, D. P. Watling. 2014. The two-regime transmission model for network loading in dynamic traffic assignment problems. *Transportmetrica A* **10** 563–584.

Boyce, D. E., B. Ran, L. Leblanc. 1995. Solving an instantaneous dynamic user-optimal route choice model. *Transport. Sci.* **29** 128–142.

Cantarella, G. E. 1997. A general fixed-point approach to multimode multi-user equilibrium assignment with elastic demand. *Transport. Sci.* **31** 107–128.

Carey, M., D. Watling. 2012. Dynamic traffic assignment approximating the kinematic wave model: System optimum, marginal costs, externalities and tolls. *Trans. Res. Part B* **46** 634–648.

Chow, A. H. F., S. Li, W. Y. Szeto, D. Z. W. Wang. 2015. Modelling urban traffic dynamics based upon the variational formulation of kinematic waves. *Transportmetrica B* **3** 169–191.

Clarka, A., A. Sumaleeb, S. Shepherda, R. Connors. 2009. On the existence and uniqueness of first best tolls in networks with multiple user classes and elastic demand. *Transportmetrica* **5** 141–157.

Daniele, P., G. Idone, A. Maugeri. 2003. Variational inequalities and the continuum model of transportation problem. *Int. J. Nonlin. Sci. Num.* **4** 11–16.

Du, J., S. C. Wong, C. W. Shu, T. Xiong M. P. Zhang, K. Choi. 2013. Revisiting Jiang's dynamic continuum model for urban cities. *Trans. Res. Part B* **56** 96–119.

Friesz, T. L., T. Kim, C. Kwon, M. A. Rigdon. 2010. Approximate network loading and dual-time-scale dynamic user equilibrium. *Trans. Res. Part B* **45** 176–207.

Friesz, T. L., A. Meimand. 2014. A differential variational inequality formulation of dynamic network user equilibrium with elastic demand. *Transportmetrica A* **10** 661–668.

Fukui, M., Y. Ishibashi. 2010. Two-dimensional city traffic model with periodically placed blocks. *Physica A* **389** 3613–3618.

Ghali, M. O., M. J. Smith. 1995. A model for the dynamic system optimum traffic assignment problem. *Trans. Res. Part B* **29** 155–170.

Han, L., S. Ukkusuri, K. Doan. 2011. Complementarity formulations for the cell transmission model based dynamic user equilibrium with departure time choice, elastic demand and user heterogeneity. *Trans. Res. Part B* **45** 1749–1767.

Ho, H. W., S. C. Wong, B. P. Y. Loo. 2006. Combined distribution and assignment model for a continuum traffic equilibrium problem with multiple user classes. *Trans. Res. Part B* **40** 633–650.

Ho, H. W., S. C. Wong, A. Sumalee. 2013. A congestion-pricing problem with a polycentric region and multi-class users: A continuum modeling approach. *Transportmetrica* **9** 514–545.

Hoogendoorn, S. P., P. H. L. Bovy. 2000. Continuum modeling of multiclass traffic flow. *Trans. Res. Part B* **34** 123–146.

Hoogendoorn, S. P., P. H. L. Bovy. 2004. Dynamic user-optimal assignment in continuous time and space. *Trans. Res. Part B* **38** 571–592.

Hoogendoorn, S. P., W. Daamen. 2005. Pedestrian behavior at bottlenecks. *Transport. Sci.* **39** 147–159.

Huang, L., S. C. Wong, M. P. Zhang, C. W. Shu, W. H. K. Lam. 2009. Revisiting Hughes' dynamic continuum model for pedestrian flow and the development of an efficient solution algorithm. *Trans. Res. Part B* **43** 127–141.

Jiang, Y. Q., S. C. Wong, H. W. Ho, P. Zhang, R. X. Liu, A. Sumalee. 2011. A dynamic traffic assignment model for a continuum transportation system. *Trans. Res. Part B* **45** 343–363.

Jiang, Y. Q., S. C. Wong, P. Zhang, R. X. Liu, Y. L. Duan, K. Choi. 2012. Numerical simulation of a continuum model for bi-directional pedestrian flow. *Appl. Math. Comput.* **218** 6135–6143.

Jiang, Y. Q., T. Xiong, S. C. Wong, C. W. Shu, P. Zhang, M. P. Zhang, W. H. K. Lam. 2009. A reactive dynamic continuum user equilibrium model for bi-directional pedestrian flows. *Acta Math. Sci.* **29B** 1541–1555.

Lam, W. H. K., H. J. Huang. 1995. Dynamic user optimal traffic assignment model for many to one travel demand. *Trans. Res. Part B* **29** 243–259.

Levin, M. W., S. D. Boyles, Nezamuddin. 2015. Warm-starting dynamic traffic assignment with static solutions. *Transportmetrica B* **3** 99–113.

Li, J., O. Fujiwara, S. Kawakami. 2000. A reactive dynamic user equilibrium model in network with queues. *Trans. Res. Part B* **34** 605–624.

Nagurney, A., J. Dong. 2002. A multiclass, multicriteria traffic network equilibrium model with elastic demand. *Trans. Res. Part B* **36** 445–469.

Potts, R. B., R. M. Oliver. 1972. *Flows in Transportation Networks*. Academic Press, New York and London.

Qian, J., Y. T. Zhang, H. K. Zhao. 2007. Fast sweeping methods for Eikonal equations on triangular meshes. *SIAM J. Numer. Anal.* **45** 83–107.

Rossa, F. D., C. DAngelo, A. Quarteroni. 2010. A distributed model of traffic flows on extended regions. *Netw. Heterog. Media* **5** 525–544.

Ryu, S., A. Chen, K. Choi. 2014. A modified gradient projection algorithm for solving the elastic demand traffic assignment problem. *Comput. Oper. Res.* **47** 61–71.

Saumtally, T., J. P. Lebacque, H. Haj-Salem. 2013. A dynamical two-dimensional traffic model in an anisotropic network. *Netw. Heterog. Media* **8** 663–684.

Shu, C. W., S. Osher. 1988. Efficient implementation of essentially non-oscillatory shock-capturing schemes. *J. Comput. Phys.* **77** 439–471.

Szeto, W. Y., H. K. Lo. 2004. A cell-based simultaneous route and departure time choice model with elastic demand. *Trans. Res. Part B* **38** 593–612.

Tao, Y. Z., Y. Q. Jiang, J. Du, S. C. Wong, P. Zhang, Y. H. Xia, K. Choi. 2014. Dynamic system-optimal traffic assignment for a city using the continuum modeling approach. *J. Adv. Transport.* **48** 782–797.

Tong, C. O., S. C. Wong. 2000. A predictive dynamic traffic assignment model in congested capacity-constrained road networks. *Trans. Res. Part B* **34** 625–644.

Wie, B. W. 1991. Dynamic analysis of user-optimized network flows with elastic travel demand. *Transport. Res. Rec.* **1328** 81–87.

Wie, B. W., T. L. Friesz, R. L. Tobin. 1990. Dynamic user optimal traffic assignment on congested multi-destination networks. *Trans. Res. Part B* **24** 431–442.

Wong, S. C. 1998. Multi-commodity traffic assignment by continuum approximation of network flow with variable demand. *Trans. Res. Part B* **32** 567–581.

Xia, Y. X., S. C. Wong, M. P. Zhang, C. W. Shu, W. H. K. Lam. 2008. An efficient discontinuous galerkin method on triangular meshes for a pedestrian flow model. *Int. J. Numer. Meth. Eng.* **76** 337–350.

Xu, M., Z. Y. Gao. 2007. Behaviours in a dynamical model of traffic assignment with elastic demand. *Chin. Phys.* **16** 1608–1614.

Xu, X. D., A. Chen, Z. Zhou, L. Cheng. 2014. A multi-class mean-excess traffic equilibrium model with elastic demand. *J. Adv. Transp.* **48** 203–222.

Yang, H. 1997. Sensitivity analysis for the elastic-demand network equilibrium problem with applications. *Trans. Res. Part B* **31** 55–70.

Yang, H., R. Kitamura, P. Jovanis, K. M. Vaughn, M. A. Abdel-Aty. 1993. Exploration of route choice behavior with advanced traveler information using neural network concept. *Transportation* **20** 199–223.

Yang, H., S. C. Wong. 2000. A continuous equilibrium model for estimating market areas of competitive facilities with elastic demand and market externalities. *Transport. Sci.* **34** 216–227.

Yin, J., S. C. Wong, N. N. Sze, H. W. Ho. 2013. A continuum model for housing allocation and transportation emission problems in a polycentric city. *Int. J. Sust. Transp.* **7** 275–298.

Zhang, P., R. X. Liu, S. C. Wong, S. Q. Dai. 2006. Hyperbolicity and kinematic waves of a class of multi-population partial differential equations. *Eur. J. Appl. Math.* **17** 171–200.

Ziliaskopoulos, A. K. 2000. A linear programming model for the single destination system optimum dynamic traffic assignment problem. *Transport. Sci.* **34** 37–49.